

Materials Degradation and Failures Series

Materials and Failures in MEMS and NEMS

Edited by **Atul Tiwari and Baldev Raj**

 **Scrivener
Publishing**

WILEY

Contents

[Cover](#)

[Half Title page](#)

[Title page](#)

[Copyright page](#)

[Preface](#)

[**Chapter 1: Carbon as a MEMS Material**](#)

[1.1 Introduction](#)

[1.2 Structure and Properties of Glassy Carbon](#)

[1.3 Fabrication of C-MEMS Structures](#)

[1.4 Integration of C-MEMS Structures with Other Materials](#)

[1.5 Conclusion](#)

[References](#)

[**Chapter 2: Intelligent Model-Based Fault Diagnosis of MEMS**](#)

[2.1 Introduction](#)

[2.2 Model-Based Fault Diagnosis](#)

[2.3 Self-Tuning Estimation](#)

[References](#)

Chapter 3: MEMS Heat Exchangers

[3.1 Introduction](#)

[3.2 Fundamentals of Thermodynamics, Fluid Mechanics, and Heat Transfer](#)

[3.3 MEMS Heat Sinks](#)

[3.4 MEMS Heat Pipes](#)

[3.5 Two-Fluid MEMS Heat Exchanger](#)

[3.6 Need for Microscale Internal Flow Passages](#)

[Nomenclature](#)

[Greek Alphabets](#)

[Subscripts](#)

[References](#)

Chapter 4: Application of Porous Silicon in MEMS and Sensors Technology

[4.1 Introduction](#)

[4.2 Porous Silicon in Biosensors](#)

[4.3 Porous Silicon for Pressure Sensors](#)

[4.4 Conclusion](#)

[References](#)

Chapter 5: MEMS/NEMS Switches with Silicon to Silicon (Si-to-Si) Contact Interface

[5.1 Introduction](#)

[5.2 Bi-Stable CMOS Front End Silicon Nanofin \(SiNF\) Switch for Non-volatile Memory Based On](#)

[Van Der Waals Force](#)

[5.3 Vertically Actuated U-Shape Nanowire NEMS Switch](#)

[5.4 A Vacuum Encapsulated Si-to-Si MEMS Switch for Rugged Electronics](#)

[5.5 Summary](#)

[References](#)

[Chapter 6: On the Design, Fabrication, and Characterization of cMUT Devices](#)

[6.1 Introduction](#)

[6.2 cMUT Design and Finite Element Modeling Simulation](#)

[6.3 cMUT Fabrication and Characterization](#)

[6.4 Summary and Conclusions](#)

[Acknowledgments](#)

[References](#)

[Chapter 7: Inverse Problems in the MEMS/NEMS Applications](#)

[7.1 Introduction](#)

[7.2 Inverse Problems in the Micro/Nanomechanical Resonators](#)

[7.3 Inverse Problems in the MEMS Stiction Test](#)

[Acknowledgment](#)

[References](#)

[Chapter 8: Ohmic RF-MEMS Control](#)

[8.1 Introduction](#)
[8.2 Charge Drive Control \(Resistive Damping\)](#)
[8.3 Hybrid Drive Control](#)
[8.4 Control Under High-Pressure Gas Damping](#)
[8.5 Comparison between Different Control Modes](#)
[References](#)

Chapter 9: Dynamics of MEMS Devices

[9.1 Introduction](#)
[9.2 Modeling and Simulation](#)
[9.3 Fabrication Methods](#)
[9.4 Characterization](#)
[9.5 Device Failures](#)
[Acknowledgments](#)
[References](#)

Chapter 10: Buckling Behaviors and Interfacial Toughness of a Micron-Scale Composite Structure with a Metal Wire on a Flexible Substrate

[10.1 Introduction](#)
[10.2 Buckling Behaviors of Constantan Wire under Electrical Loading](#)
[10.3 Interfacial Toughness between Constantan Wire and Polymer Substrate](#)
[10.4 Buckling Behaviors of Polymer Substrate Restricted by Constantan Wire](#)
[10.5 Conclusions](#)

[Acknowledgments](#)
[References](#)

Chapter 11: Microcantilever-Based Nano-Electro-Mechanical Sensor Systems: Characterization, Instrumentation, and Applications

[11.1 Introduction](#)
[11.2 Operation Principle and Fundamental Models](#)
[11.3 Microcantilever Sensor Fabrication](#)
[11.4 Mechanical and Electrical Characterization of Microcantilevers](#)
[11.5 Readout Principles](#)
[11.6 Application of Microcantilever Sensors](#)
[11.7 Energy Harvesting for Sensor Networks](#)
[11.8 Conclusion](#)
[References](#)

Chapter 12: CMOS MEMS Integration

[12.1 Introduction](#)
[12.2 State-of-the-Art inertial Sensor](#)
[12.3 Capacitance Sensing Techniques](#)
[12.4 Capacitance Sensing Architectures](#)
[12.5 Continuous Time Voltage Sensing Circuit](#)
[12.6 CMOS ASIC Design](#)
[12.7 Test Results of CMOS-MEMS Integration](#)
[12.8 Electrical Reliability Issues](#)
[References](#)

Chapter 13: Solving Quality and Reliability Optimization Problems for MEMS with Degradation Data

Abbreviations

13.1 Introduction

13.2 Notations and Assumptions

13.3 Reliability Model

13.4 Numerical Example

13.5 Conclusions

References

Index

Materials and Failures in MEMS and NEMS

Scrivener Publishing
100 Cummings Center, Suite 541J
Beverly, MA 01915-6106

Materials Degradation and Failure Series

Studies and investigations on materials failure are critical aspects of science and engineering.

The failure analysis of existing materials and the development of new materials demands in-depth understanding of the concepts and principles involved in the deterioration of materials

The *Material's Degradation and Failure* series encourages the publication of titles that are centered on understanding the failure in materials. Topics treating the kinetics and mechanism of degradation of materials is of particular interest. Similarly, characterization techniques that record macroscopic (e.g., tensile testing), microscopic (e.g., *in-situ* observation) and nanoscopic (e.g., nanoindentation) damages in materials will be of interest. Modeling studies that cover failure in materials will also be included in this series.

Series Editors: Atul Tiwari and Baldev Raj

Dr. Atul Tiwari, CChem
Director, R&D, Pantheon Chemicals
225 W. Deer Valley Road #4
Phoenix, AZ 85027 USA

Email: atulmrc@yahoo.com, atiwari@pantheonchemical.com

Dr. Baldev Raj, FTWAS, FNAE, FNA, FASc, FNASc
Director, National Institute of Advanced Studies
Indian Institute of Science Campus
Bangalore 560 012, India

Email: baldev.dr@gmail.com, baldev_dr@nias.iisc.ernet.in

Publishers at Scrivener

Martin Scrivener(martin@scrivenerpublishing.com)
Phillip Carmical (pcarmical@scrivenerpublishing.com)

Materials and Failures in MEMS and NEMS

Edited by

Atul Tiwari and Baldev Raj



WILEY

Copyright © 2015 by Scrivener Publishing LLC. All rights reserved.

Co-published by John Wiley & Sons, Inc. Hoboken, New Jersey and Scrivener Publishing LLC, Salem, Massachusetts. Published simultaneously in Canada.

No part of this publication may be reproduced, stored in a retrieval system, or transmitted in any form or by any means, electronic, mechanical, photocopying, recording, scanning, or otherwise, except as permitted under Section 107 or 108 of the 1976 United States Copyright Act, without either the prior written permission of the Publisher, or authorization through payment of the appropriate per-copy fee to the Copyright Clearance Center, Inc., 222 Rosewood Drive, Danvers, MA 01923, (978) 750-8400, fax (978) 750-4470, or on the web at www.copyright.com. Requests to the Publisher for permission should be addressed to the Permissions Department, John Wiley & Sons, Inc., 111 River Street, Hoboken, NJ 07030, (201) 748-6011, fax (201) 748-6008, or online at <http://www.wiley.com/go/permission>.

Limit of Liability/Disclaimer of Warranty: While the publisher and author have used their best efforts in preparing this book, they make no representations or warranties with respect to the accuracy or completeness of the contents of this book and specifically disclaim any implied warranties of merchantability or fitness for a particular purpose. No warranty may be created or extended by sales representatives or written sales materials. The advice and strategies contained herein may not be suitable for your situation. You should consult with a professional where appropriate. Neither the publisher nor author shall be liable for any loss of profit or any other commercial damages, including but not limited to special, incidental, consequential, or other damages.

For general information on our other products and services or for technical support, please contact our Customer Care Department within the United States at (800) 762-2974, outside the United States at (317) 572-3993 or fax (317) 572-4002.

Wiley also publishes its books in a variety of electronic formats. Some content that appears in print may not be available in electronic formats. For more information about Wiley products, visit our web site at www.wiley.com.

For more information about Scrivener products please visit www.scrivenerpublishing.com.

Library of Congress Cataloging-in-Publication Data:

Materials and failures in MEMS and NEMS / edited by Atul Tiwari and Baldev Raj.

1 online resource.

Includes bibliographical references and index.

Description based on print version record and CIP data provided by publisher; resource not viewed.

ISBN 978-1-119-08387-0 (pdf) – ISBN 978-1-119-08386-3 (epub) – ISBN 978-1-119-08360-3 (cloth : alk. paper)

1. Microelectromechanical systems–Design and construction. 2. Nanoelectromechanical systems–Design and construction. I. Tiwari, Atul, editor. II. Raj, Baldev, 1947–editor.

TK7875

621.381–dc23

2015027730

ISBN 978-1-119-08360-3

Preface

Manufacturing, diagnosis and treatment of biospecies, agriculture, energy and infrastructure, governance, security, etc., need sensors and devices based on well-grounded concepts, engineering and technology. Miniaturization demands new materials, designs and fabrication technologies. The decrease in the size and volume of devices has necessitated the incorporation of a high level of fabrication technologies. There is a priority need to address failures in micro- and nanodevices.

The invention of Microelectromechanical Systems (MEMS) and Nanoelectromechanical Systems (NEMS) fabrication technologies has revolutionized the science and engineering industry. It is estimated that market prospects for MEMS and NEMS will increase rapidly to reach \$200 billion in 2025. The key to the success of MEMS and NEMS will be the development of technologies that can integrate multiple devices with electronics on a single chip. Among the technologies available so far, the fabrication of MEMS and/or NEMS has been predominately achieved by etching the polysilicon material. Novel materials and technologies are being explored to overcome the challenges in fabrication or manufacturing processes. In order to meet the ever-increasing demands of MEMS and NEMS, enormous amounts of research, applications and innovations have been explored and exploited. Most of the relevant information originating from such efforts is being treated as confidential or privileged, which seeds extensive barriers to the research, development and aspirational demands of these technologies.

This book includes chapters written by eminent experts in the area of MEMS and NEMS. The opening chapter of this book reviews various C-MEMS fabrication technologies

involving patterning of polymeric precursors of carbon such as epoxy photoresists and sol-gel polymers, followed by pyrolysis to generate glassy or semicrystalline carbon. Another chapter discusses the origins of fault in such devices, related mathematical models and utilization of filters in fault diagnosis. Also, the authors have illustrated the structure of a multiple-model adaptive estimator and its application in fault diagnosis simulation. Another chapter provides an overview of the design of MEMS heat exchangers such as heat sinks, heat pipes and two-fluid heat exchangers. The formation of porous silicon devices by electrochemical etching of silicon and the control over the porosity and pore size are discussed in a separate chapter. The use of such porous silicon devices as biosensors is thoroughly investigated by these contributors. Further, a chapter provides an overview on MEMS and NEMS switches using Si-to-Si contact. An interesting chapter discusses the design challenges during fabrication and failure analysis of cMUT devices. Investigators have compared the device fabrication by surface micromachining and wafer bonding techniques. Moreover, failure analysis of cMUT using various materials characterization techniques and their importance for successful device fabrication are also investigated.

A successive chapter investigates an effective approach to solve inverse problems in MEMS and NEMS. This chapter describes inverse problems in micro- and nanomechanical resonators and also the stiction test of MEMS and NEMS. Further, there is a chapter in the book dedicated to the control of ohmic RF-MEMS switches operating under different actuation modes, such as single pulse, tailored pulse, and tailored-pulse optimization methods, based on Taguchi's technique of resistive damping; and the hybrid actuation mode, which is a combination of the tailored pulse, the resistive damping, and Taguchi's optimization technique. Additional challenges involved in design methodologies, and available simulation packages to model and simulate MEMS devices are explored in a separate chapter. To develop MEMS devices and to understand the inception of fabrication defects, researchers have explored fabrication techniques such as surface micromachining and bonding silicon to glass. The use of different characterization techniques, such as visual, electrical and mechanical, for inspecting the defects in these devices has also been demonstrated. An independent chapter systematically investigates the buckling behavior of a typical micron-scale constantan-wire/polymer-substrate structure under electrical loading. Another crucial chapter discusses many important aspects of microcantilever sensors such as operation principles, fabrication of silicon and polymer microcantilevers, mechanical and electrical characterization, readout principles, applications of microcantilever sensors for vapor-phase chemical or gas detection, biosensing and agriculture applications; and nanogenerators for energy harvesting. A chapter in the book elaborates the inherent challenges encountered in CMOS-MEMS along with the possibility of integration at board and chip levels. This chapter also lists various circuit architectures being used in capacitance detection along with a detailed comparison on their merits and demerits.

The final chapter proposes a mathematical model to determine strategies for preventive replacement and inspection for MEMS that are subject to multiple dependent competing failure processes as a result of degradation and/or shock loads.

We are confident that this book will constitute a large knowledge bank for students, research scholars and engineers who are involved in the research, development and deployment of advanced MEMS and NEMS for a wide variety of applications. To the best of the editors' knowledge, such a book that addresses the developments and failures in these advanced devices has not yet been available to readers. Comprehensive expertise is mapped out and discussed in this book to advance the knowledge bank of readers in order to enable precise control over dimensional stability, quality, reliability, productivity and life cycle management of MEMS and NEMS.

The editors look forward to constructive suggestions and feedback for improving the next edition of this book on this important, relatively young subject of increasing importance and relevance.

Wishing you a purposeful and wonderful reading experience.

Atul Tiwari, PhD
Baldev Raj, PhD
August 4, 2015

Chapter 1

Carbon as a MEMS Material

Amritha Rammohan* and Ashutosh Sharma

Department of Chemical Engineering, Indian Institute of Technology, Kanpur, Uttar Pradesh, India

**Corresponding authors: r.amritha@gmail.com*

Abstract

Carbon has become a popular material in microelectromechanical (MEMS) applications because of its versatile electrochemical and mechanical properties, as well as the numerous precursor materials and facile fabrication methods available. This review details various C-MEMS fabrication technologies, most of which involve the patterning of polymeric precursors of carbon such as epoxy photoresists and sol-gel polymers followed by their pyrolysis to create glassy or semicrystalline carbon pattern replicas. The structure and properties of glassy carbon, as well as the pyrolysis process and concurrent shrinkage, are also discussed in detail, as these directly affect the applicability of the carbon structures and devices. The integration of carbon structures in MEMS devices by means of surface modification and the incorporation of additives and fillers such as carbon nanotubes and carbon nanofibers to enhance the functional properties are also discussed.

Keywords: Carbon, C-MEMS, pyrolysis, volumetric shrinkage, MEMS integration, lithography

1.1 Introduction

Carbon is one of the most versatile materials in the periodic table. Due to its ability to form sp , sp^2 , and sp^3 hybridized covalent bonds with various elements including itself, carbon-based compounds and materials are amongst the most adaptable materials available to us. The ability of carbon to form bonds with itself is manifested in the form of many allotropes of carbon including fullerenes, nanotubes, graphite, graphene, and diamond. Even within these allotropes, despite being all made of carbon, the properties such as electrical conductivity, hardness, and strength vary widely with allotrope due to different microstructures in terms of crystallite size, long-range order, anisotropy, *etc.* [1]. Amorphous or glassy carbon, in particular, has a wide window of electrochemical stability as well as high thermal conductivity and excellent biocompatibility, warranting its use in various electrochemical and biological applications [2]. Diamond-like carbon or DLC, another form of carbon, has superior tribological properties and wear resistance, and anisotropic carbon materials such as nanotubes and nanofibers can be leveraged for their unique and anisotropic electromechanical properties as well [2-4].

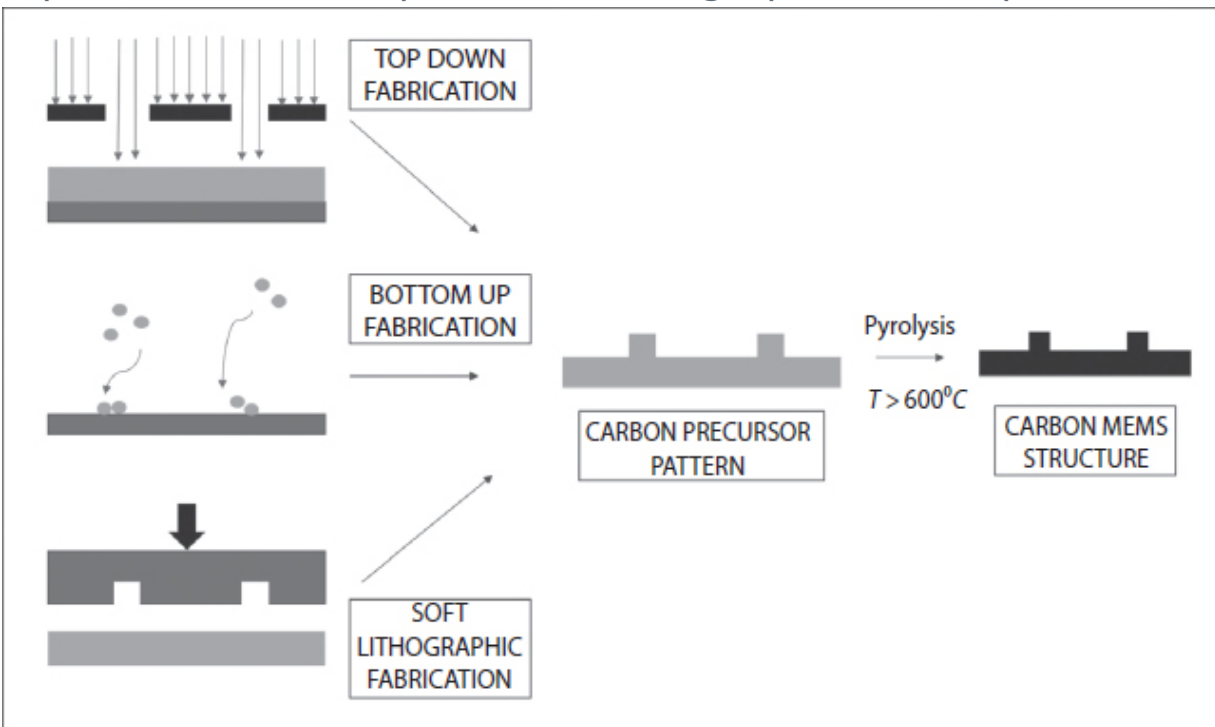
When this versatility in functional properties is combined with appropriate micro/nanofabrication techniques, carbon structures become highly viable as elements in micro and nano electromechanical systems (MEMS/NEMS). In order to create micro- and nanosized electromechanical structures such as actuators and microsensors from carbon, appropriate robust and facile micro/nanofabrication techniques have to be adopted. The methods to pattern carbon and its precursors into MEMS structures are divided, like other microfabrication techniques, into top-down and bottom-up techniques. Top-down techniques are subtractive processes such as reactive ion etching (RIE) and lithographic

patterning with photons, electrons, or ions. Bottom-up or additive processes include sputtering, evaporation, and chemical vapor deposition (CVD) [5]. While top-down techniques create deterministic patterns with good shape and size control, bottom-up techniques result in increased functionality and have greater capability for three-dimensional (3D) patterns. Self-assembled structures that are formed with very little external guidance or direction also fall in the latter category of bottom-up techniques. Apart from strictly top-down and bottom-up techniques, many fabrication techniques include a combination of these two. For example, hierarchical structures can be achieved by top-down patterning of large-scale structures and bottom-up patterning of smaller, 3D features. Soft lithographic techniques such as micromolding and nanoimprinting are often considered a third classification of microfabrication techniques and have also been used successfully in the patterning of C-MEMS (Carbon MEMS) structures [6].

One process that facilitates the fabrication of amorphous or glassy carbon microstructures involves the pyrolysis of carbon-containing precursor molecules (usually polymers) that have been prefabricated into requisite micro/nanostructures ([Figure 1.1](#)). Pyrolysis or carbonization is the method of heating carbon-containing precursors to temperatures upward of 600 °C in an inert atmosphere such as nitrogen or argon to remove noncarbonaceous components in a material by volatilizing them into gaseous and hence removable compounds. This method, apart from allowing the creation of any required shape as long as appropriate formable precursors are used, also allows tweaking the properties of the final carbon micro/nanostructures by the rational use of various precursors with different functional groups. Appropriate precursors are those carbon-containing polymers that result

in a high enough yield of carbonaceous residue and at the same time do not reflow when subjected to high temperatures during pyrolysis [2]. Thus, the methods to create glassy carbon MEMS structures can be decoupled into various methods to create microstructures in appropriate precursors and the pyrolysis processes ([Figure 1.1](#)).

Figure 1.1 Fabrication of Carbon MEMS structures using top-down, bottom-up and soft lithographic techniques.



This review is structured as follows. Due to the fact that majority of C-MEMS/NEMS processes involve polymer-derived amorphous or semicrystalline carbon, its properties are reviewed and contrasted with other MEMS materials. The process of pyrolysis for the carbonization is discussed in detail along with methods to address the issue of shrinkage. Then, lithographic techniques and their capabilities and modifications for C-MEMS/NEMS fabrication are discussed. This is followed by a description of bottom-up techniques, in particular self-assembly techniques for C-MEMS/NEMS. Soft

lithographic techniques are also briefly covered. Finally, additives and surface modification techniques to improve and expand the applicability of carbon are examined.

1.2 Structure and Properties of Glassy Carbon

Glassy carbon is typically a hard solid prepared by treating polymeric precursors such as copolymer resins at elevated temperatures (600–3000 °C) having increasing amount of graphitic content with increasing temperature. The high temperature removes almost all of the noncarbon elements present in the polymers leaving behind a carbonaceous residue. A fully graphitic material does not develop in usual pyrolysis due to the difficulty in breaking the C–C bonds in the parent polymeric chains as well as other factors such as ratio of sp^2 to sp^3 carbon atoms and amount of hydrogen present in the precursor. The structure is generally understood as entangled ribbons of graphitic planes containing small isolated crystals of graphite. When characterized by Raman spectroscopy, two first-order bands around 1360 cm^{-1} (D band) and 1580 cm^{-1} (G band) are usually observed, which indicate the defect-induced, double-resonance scattering and symmetry in-plane stretching of graphite, respectively. Weak second-order bands related to the 3D ordering of graphite may also be observed between 2700 and 2900 cm^{-1} . It is important to note that the D band mainly arises due to the finite graphite crystallite size and associated defects [7]. As glassy carbon contains smaller crystallites of graphite, its density is less than that of graphite and can be applied in applications

requiring lightweight yet chemically inert or thermally stable materials.

While the different preparation methods result in a range of physical properties of glassy carbon, it does have many advantages as a MEMS material. Glassy carbon, for instance, has a lower Young's modulus compared to silicon (10–40 GPa compared to 40–190 GPa for silicon) and a lower surface energy. Thus, carbon can be used in MEMS actuators or other devices where high stiffness is detrimental. The lower surface energy of carbon also solves the problem of stiction in contacting or proximal MEMS elements where capillary forces cause sticking between close surfaces. Carbon resulting from pyrolysis is also rather inert and impervious in many corrosive chemical environments. It is also possible to tailor the porosity and functionalize the surface of glassy carbon using various carbon chemistry routes as illustrated in Section 1.4.

Glassy carbon is also a model material or gold standard for electrochemists to compare the electrochemical properties of electrodes of other materials as it exhibits excellent electrochemical properties. The electrochemical and physical properties of photoresist material pyrolyzed at temperatures between 600 °C and 1100 °C have been studied in detail, and it has been found that resistance of the material is lower and the electrochemical performance of the carbon material is often found to be better. The pyrolyzed positive photoresist (*eg.* AZ 4330) films have low capacitance as well as background current [8].

Apart from glassy carbon, other carbon-based materials such as DLC, carbon nanotubes (CNTs), and carbon nanofibers (CNFs) have also been applied to great benefit in MEMS devices. However, these materials often lack the capability to form the entire MEMS device by themselves due to fabrication and manipulation constraints. For instance, while DLC is particularly useful as a coating

material to improve the wear resistance, reduce friction, and stiction in contacting microcomponents in MEMS devices, the residual stresses that are created in most of the high-energy techniques involved in DLC fabrication often lead to delamination of thicker DLC films precluding their use as structural elements [3]. CNTs and CNFs have unique and anisotropic thermal and electrochemical properties and have been used as structural elements such as cantilevers and microsensors. However, the manipulation and assembly of fabricated CNTs and CNFs on MEMS devices are nontrivial due to the possibility of physical damage or morphological changes occurring. Cook and Carter [9] have recently reviewed the effect of different MEMS processes on arc-discharge produced and catalytically grown multiwall CNTs (MWCNTs) and found that while CVD deposition of other materials is compatible with MWCNTs, plasma etching processes tend to cause significant damage. Dau *et al.* [10] have been able to manually maneuver CVD-grown CNT films onto a substrate and pattern it using e-beam lithography into a mechanical sensor. It is also possible to directly synthesize patterned CNT structures for MEMS applications by methods such as CVD on patterned catalyst substrates [11–14], direct or post-synthetic patterning [15–18], templated deposition [19], *etc.* The incorporation of CNTs and CNFs into C-MEMS devices can be as fillers or (surface) additives to enhance useful properties or as structural elements integrated with the rest of the device. Both these uses are discussed in Section 1.4.

1.3 Fabrication of C-MEMS Structures

1.3.1 Mechanism and Features of the Pyrolysis Process

As most C-MEMS processes involve the use of pyrolysis, also known as carbonization, for the conversion of precursors to carbon, a good understanding of this process is a prerequisite for understanding C-MEMS fabrication. Pyrolysis, from the Greek for fire (*pyro*) and separation (*lysis*), is the thermochemical decomposition of a material and in the context of carbonization refers to the breakdown of carbon-containing precursors at elevated temperatures in an inert or reducing environment. As early as the 1970s, carbon-containing polymers such as phenol formaldehyde, polyacrylonitrile (PAN), and polyimide have been pyrolyzed to amorphous carbon and their electrical properties studied. Jenkins and Kawamura [20] were amongst the first to study the process of pyrolyzing polymers into glassy carbon, where the polymers do not go through a plastic or reflow phase. They have classified the pyrolysis mechanism into four typical stages:

- i.** Around 300 °C - pre-carbonization stage - polymer turns black.
- ii.** 300-500 °C - carbonization stage - elements such as nitrogen and oxygen are removed from the material.
- iii.** 500-1200 °C - dehydrogenation stage - gradual elimination of hydrogen.
- iv.** 1200 °C and above - annealing stage.

As mentioned earlier, the graphitization of the carbon also occurs when pyrolyzing at elevated temperatures with percentage graphitization increasing with increasing temperatures. At pyrolysis temperatures between 2500 °C and 3300 °C, it is assumed that all nongraphitic regions are annealed out resulting in a near-complete graphitization of

the material. Hence, this regime is referred to as graphitization regime.

In the case of lithography-based C-MEMS structures, both positive and negative polymeric photoresists can be used as carbon precursors and have the potential to be carbonized after patterning ([Table 1.1](#)). Hsia *et al.* [27] have researched the formation of carbon from SPR-220 (positive photoresist), by heating in Ar atmosphere to 900 °C followed by a second annealing step in a H₂/Ar (reducing) mixture. It was found that this results in a porous carbon with a high surface area, which has been applied as a supercapacitor electrode material for energy storage applications. Negative photoresists, such as SU-8, on the other hand, have a tendency to burn due to the dissolved oxygen present within them [39]. Thicker films of negative photoresist-derived carbon structures can also delaminate from silicon substrate and require ameliorative measures such as slow heating during pyrolysis to minimize thermal stresses and/or an intermediate layer to improve adhesion.

Table 1.1. Representative list of carbon precursors.

Material	Chemical composition and properties	Patterning method	References
SU-8	Epoxy resin, negative photoresist	Photolithography, interference lithography, electrospinning	[2, 21, 22] <i>etc.</i>
Novolac resin	Phenol formaldehyde polymer	Photolithographic patterning	[23]
EPON SU2.5	Bisphenol-A type novolac epoxy	Photolithographic patterning	[24, 25]
AZ 9260, AZ 4330, <i>etc.</i>	Polymeric resins containing di-azo compounds, positive photoresists	Photolithographic patterning	[26]
SPR 220	Cresol novolac resin and ethyl lactate	Photolithographic patterning	[27]
SC-100	Conventional cyclic polyisoprene photoresist	Photolithographic patterning and buckling-instability-induced patterning	[28]
KMPR 1050	Epoxy, negative photoresist	Photolithographic patterning	[29]
PMMA	Poly methyl methacrylate, e-beam resist	Electron-beam lithography and simultaneous carbonization	[30–32]
Resorcinol diglycidil ether and derivatives	Epoxy resin	Two photon lithography, 3D microtransfer molding	[33]
Copolymers of furfuryl alcohol–phenol	Phenolic resin	Micromolding in capillaries, microtransfer molding	
Resorcinol formaldehyde		Sol–gel, microtransfer molding	[34–36]
Polymer Cirlex	Polyimide	Lithographic patterning	[37]
Parylene	Poly-(p-xylylene)	CVD	[38]

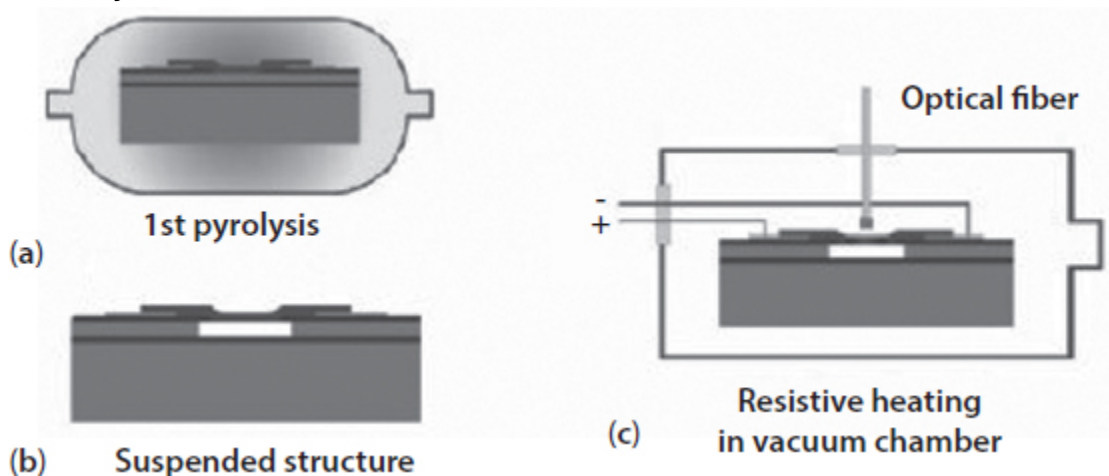
One of the most salient features of the pyrolysis process is the volumetric shrinkage that accompanies it. While this shrinkage can be advantageous in reducing the dimensions of realizable structures [36], it can cause defects such as buckling in constrained structures. In bulk or block structures, where the entire part is unconstrained and shrinks isotropically, the buckling is minimal, however, in the case of devices involving C-MEMS structures integrated with other materials or on a substrate, this is an issue. In self-assembled structures such as xerogels and aerogels, the random orientation and open structure allow their shrinkage and expansion during processing steps such as pyrolysis [40]. Much research has gone into optimizing the pyrolysis process to reduce the defects such as buckling, cracking, and delamination that occur as a result of thermal and shrinkage-related stresses.

To address the issue of shrinkage and related stresses, creating an optimal pyrolysis protocol by modifying heating and cooling rates, temperature of pyrolysis and the atmosphere of carbonization is one of the solutions, and modifying the carbon precursor material with filler material, *etc.*, and creating patterns with lower possibility of buckling are other techniques. Tang *et al.* [41] have utilized a three-step linear pyrolysis method as well as a mechanical interlocking step, the latter to achieve better bonding and prevent delamination. Naka *et al.* [42] have approached the problem of high-temperature pyrolysis by employing a resistive heating process as the last step of the pyrolysis of a polymeric microstructure on silicon structure. This resistive self-heating is achieved by means of a microheater designed into the microstructure of photosensitive polyimide ([Figure 1.2](#)). After initial pyrolysis step, a current is applied to the microheater to complete the carbonization by resistive heating. Since the polymeric structure

carbonizes itself by self-heating, the thermal damage of other materials in the MEMS device is prevented.

Figure 1.2 Schematic diagram of multistep pyrolysis (a) Preliminary pyrolysis using a quartz furnace (b) fabrication of suspended polymer microstructure, and (c) resistive heating in a vacuum chamber as final pyrolysis. The optical fiber is used to observe the microheater element during resistive heating.

(Reproduced with permission from [42]. Copyright 2008 The Japan Society of Applied Physics)



Wang *et al.* [21] have illustrated a dual use of the pyrolysis process by using a two-step pyrolysis technique with forming gas [H_2 (5%)/ N_2 mixture] at 900°C as a second step to cause the local CVD of CNFs from gases emanating from the polymer during pyrolysis. A gold layer coated on the substrate on which modified SU-8 photoresist was patterned was converted into gold nanoballs at the base of carbon posts. It is also possible to exploit the shrinkage during pyrolysis to create unique shapes as has been shown by deVolder *et al.* [2] who have created canopy shapes connecting carbon pillars by intentionally fabricating an SU-8 topping layer that shrinks and pulls the pillars together as shown in [Figure 1.2](#).

While shrinkage is one of the aspects of pyrolysis, the pyrolysis conditions also affect the functional properties of

the MEMS structures. For example, faster heating rates increase the porosity of the pyrolyzed carbon. Teixidor *et al.* [43] have evaluated the effect of pyrolysis conditions on the battery characteristics of a pillar array of epoxy resin and found that pyrolysis at higher temperatures and slower ramping up schedules reduce the irreversible capacity of the carbon electrodes illustrated in [Figure 1.3](#).

[Figure 1.3](#). Examples of intricate amorphous carbon microarchitectures. (a) FEM simulation and SEM images of the 3D carbon microarchitecture formation by the directed shrinkage of an SU-8 topping layer during pyrolysis. (b) SEM images of six- and 12-legged 3D geometries. Left and right images have a different tilt angle, which is controlled by the pillar height. (c) 3D circular bridge with six legs and integrated pyrolyzed carbon bottom electrodes. (d) 3D arrangement of 180 legs connecting a suspended carbon sheet to interdigitated bottom electrodes.

(Adapted with permission from [2], Copyright 2011 American Chemical Society.)